INTERFACE

rsif.royalsocietypublishing.org

Research

Cite this article: Bellini C *et al*. 2017 Comparison of 10 murine models reveals a distinct biomechanical phenotype in thoracic aortic aneurysms. *J. R. Soc. Interface* **14**: 20161036.
http://dx.doi.org/10.1098/rsif.2016.1036

Received: 21 December 2016
Accepted: 18 April 2017

Subject Category:
Life Sciences–Engineering interface

Subject Areas:
bioengineering, biomechanics

Keywords:
fibrillin-1, fibulin-4, 5, actomyosin, transforming growth factor-β, tuberous sclerosis complex-1, angiotensin II

Author for correspondence:
J. D. Humphrey
e-mail: jay.humphrey@yale.edu

†C.B., M.R.B. and A.W.C. contributed equally.

Electronic supplementary material is available online at https://dx.doi.org/10.6084/m9.figshare.c.3757226.

THE ROYAL SOCIETY PUBLISHING

Comparison of 10 murine models reveals a distinct biomechanical phenotype in thoracic aortic aneurysms

C. Bellini[1,†], M. R. Bersi[1,†], A. W. Caulk[1,†], J. Ferruzzi[1], D. M. Milewicz[2], F. Ramirez[3], D. B. Rifkin[4,5], G. Tellides[6,7], H. Yanagisawa[8] and J. D. Humphrey[1,7]

[1]Department of Biomedical Engineering, Yale University, New Haven, CT, USA
[2]Department of Internal Medicine, McGovern Medical School, University of Texas Health Science Center, Houston, TX, USA
[3]Department of Pharmacological Sciences, Icahn School of Medicine at Mt Sinai, New York, NY, USA
[4]Department of Cell Biology, and [5]Department of Medicine, New York University, New York, NY, USA
[6]Department of Surgery, and [7]Vascular Biology and Therapeutics Program, Yale School of Medicine, New Haven, CT, USA
[8]Life Science Center, Tsukuba Advanced Research Alliance, University of Tsukuba, Ibaraki, Japan

CB, 0000-0003-0823-4613

Thoracic aortic aneurysms are life-threatening lesions that afflict young and old individuals alike. They frequently associate with genetic mutations and are characterized by reduced elastic fibre integrity, dysfunctional smooth muscle cells, improperly remodelled collagen and pooled mucoid material. There is a pressing need to understand better the compromised structural integrity of the aorta that results from these genetic mutations and renders the wall vulnerable to dilatation, dissection or rupture. In this paper, we compare the biaxial mechanical properties of the ascending aorta from 10 murine models: wild-type controls, acute elastase-treated, and eight models with genetic mutations affecting extracellular matrix proteins, transmembrane receptors, cytoskeletal proteins, or intracellular signalling molecules. Collectively, our data for these diverse mouse models suggest that reduced mechanical functionality, as indicated by a decreased elastic energy storage capability or reduced distensibility, does not predispose to aneurysms. Rather, despite normal or lower than normal circumferential and axial wall stresses, it appears that intramural cells in the ascending aorta of mice prone to aneurysms are unable to maintain or restore the intrinsic circumferential material stiffness, which may render the wall biomechanically vulnerable to continued dilatation and possible rupture. This finding is consistent with an underlying dysfunctional mechanosensing or mechanoregulation of the extracellular matrix, which normally endows the wall with both appropriate compliance and sufficient strength.

1. Introduction

Advances in medical genetics have identified diverse mutations that predispose to thoracic aortic aneurysms (TAAs), including those that affect genes that code extracellular matrix proteins, transmembrane receptors, cytoskeletal proteins or intracellular signalling molecules [1–3]. We recently suggested that this collection of mutations implicates a common lost ability of smooth muscle cells to sense matrix-mediated mechanical stimuli (i.e. to mechanosense) and/or to organize and orient the matrix accordingly (i.e. to mechanoregulate) [4], which in turn could compromise the mechanical functionality and structural integrity of the aortic wall [5]. Ramifications of such changes are intuitive, given that the ultimate fate of a compromised thoracic aorta—dissection and rupture—arises when wall stress exceeds strength.

Some descriptors of the mechanical properties of the aorta can be inferred from *in vivo* data (e.g. distensibility or local pulse wave velocity), yet full

mechanical characterization requires *in vitro* multiaxial testing of isolated samples. There is a growing database on the material properties of excised portions of the human thoracic aorta in health and disease (e.g. [6–10]) and much has been learned. Nevertheless, no study has consistently compared properties for different mutations that predispose to TAAs, which is challenging if using human tissue. Mouse models, in contrast, can provide the data needed to quantify and compare the biaxial wall mechanics and underlying microstructure as a function of specific genetic mutations that lead to aneurysmal dilatation, dissection or rupture.

In this paper, we present the first consistent comparison of the passive biaxial mechanical properties of diverse monogenic mouse models that have been used to study thoracic aortic disease: fibrillin-1 deficient ($Fbn1^{mgR/mgR}$; [11]), smooth muscle cell-specific fibulin-4 null ($Fbln4^{SMKO}$; [12]), smooth muscle myosin heavy chain variant ($Myh11^{R247C/R247C}$; [13]), postnatal disruption of smooth muscle cell specific transforming growth factor-β receptor II (*mT/mG.Myh11-CreER*^{T2}.$Tgfbr2^{f/f}$ + Tmx or simply $Tgfbr2^{f/f}$ + Tmx, which denotes induction of the genetic mutation with tamoxifen; [14]) and postnatal disruption of smooth muscle cell-specific tuberous sclerosis complex-1 (*mT/mG.Myh11-CreER*^{T2}.$Tsc1^{f/f}$ + Tmx or $Tsc1^{f/f}$ + Tmx; unpublished). See Discussion for details of these mutations and their clinical implications. Note, too, that hypertension is a significant risk factor for TAAs. Similar analyses were thus carried out for models with induced hypertension (HT), including an apolipoprotein-E null ($ApoE^{-/-}$ + HT; [15]) and the smooth muscle myosin heavy chain variant ($Myh11^{R247C/R247C}$ + HT; [16]). The experimental data for the $Fbln4^{SMKO}$, $Tsc1^{f/f}$ + Tmx and $ApoE^{-/-}$ + HT mice are new, whereas data for the other four models were collected previously using the same methods [16–18]. For purposes of further comparison, we also include data from four different groups of controls (pooled into *Control*; [19]) and new data for acute elastase-exposure to otherwise normal ascending aorta (*Elastase*). Finally, we include previously reported data for a fibulin-5 null model that exhibits an altered microstructure and mechanical properties but no propensity to aneurysmal dilatation ($Fbln5^{-/-}$; [20,21]). Comparisons of results across these 10 models confirm that lost mechanical functionality, indicated by a reduced capability to store elastic energy or a decreased distensibility, need not lead to or indicate aneurysmal dilatation. Conversely, an inability of intramural cells (primarily smooth muscle cells and fibroblasts) to maintain the circumferential material stiffness near normal correlates with aneurysmal development, consistent with a compromised ability to mechanosense and mechanoregulate the extracellular matrix. There is, therefore, strong motivation to refocus clinical assessments towards material stiffness.

2. Methods

Detailed methods are provided in the electronic supplementary material. Briefly, all animal protocols were approved by the appropriate Institutional Animal Care and Use Committee. The ascending aorta, whether aneurysmal or not, was excised upon euthanasia and placed within a custom, computer-controlled biaxial testing system. Specimens were acclimated to the *in vitro* environment, preconditioned and subjected to seven different cyclic biaxial protocols. Associated data were analysed using a validated nonlinear constitutive relation that allowed consistent calculations of multiple mechanical metrics of importance, including mean biaxial wall stress, material stiffness and elastic energy storage or dissipation. Where appropriate, data were analysed using an analysis of variance with significance assumed at $p < 0.05$.

3. Results

Details on background, age, body mass and blood pressure are listed in table 1 for the mice that constitute the single control group, the elastase-exposure group and the eight groups with mutations or pharmacological treatments. Figure 1 compares group-specific mean structural (figure 1*a*,*b*) and material (figure 1*c*,*d*) properties as well as representative geometric (figure 1*e*–*n*) and histological (figure 1*o*–*x*) characteristics for the ascending aorta across these 10 models: *Control*, *Elastase*, $Myh11^{R247C/R247C}$, $Fbln5^{-/-}$, $Myh11^{R247C/R247C}$ + HT, $ApoE^{-/-}$ + HT, $Tgfbr2^{f/f}$ + Tmx, $Tsc1^{f/f}$ + Tmx, $Fbn1^{mgR/mgR}$ and $Fbln4^{SMKO}$. Control vessels exhibit the advantageous biaxially compliant behaviour of a healthy ascending aorta, whereas elastase-exposed vessels represent a stiff upper-bound behaviour for comparison (figure 1*c*,*d*). That is, although not meant to replicate an *in vivo* situation, acute intraluminal infusion of elastase results in a mildly dilated (figure 1*f*) and severely thinned (figure 1*p*) wall wherein nearly all elastic fibres degrade simultaneously without concomitant matrix remodelling. Hence, elastase-exposed vessels bear applied loads primarily via uncrimped adventitial collagen fibres, which results in an almost complete loss of circumferential distension (figures 1*a* and 2*a*) and axial extension (figures 1*b* and 2*b*) as well as a significant increase in circumferential material stiffness (figure 2*e*) and decrease in energy storage capability (figure 2*g*). These two groups are, therefore, good comparators for TAA models.

Despite data confirming that the smooth muscle myosin heavy chain (*MYH11*) variant R247C disrupts contraction of aortic smooth muscle cells [13], this variant has minimal effects on gross anatomy (figure 1*g*), microstructure (figure 1*q*) and mechanical behaviour (figure 1*a*–*d*) of the ascending aorta in the mouse ($Myh11^{R247C/R247C}$). Hypertension induced via a high-salt diet in combination with L-NAME can cause aortic dissections in these mice [16], but the non-dissected samples studied herein after 18 weeks of hypertension exhibit only a mild thickening of the wall (figure 1*i*,*s*) with no dramatic change in wall mechanics (figure 1*a*–*d*). Consistent with their milder (perhaps simply earlier stage disease) phenotypes (figure 1*k*,*l*) and few fragmented elastic laminae (figure 1*u*,*v*), the structural and material behaviours for the $Tgfbr2^{f/f}$ + Tmx and $Tsc1^{f/f}$ + Tmx ascending aortas are also similar to those of controls (figure 1*a*–*d*). In contrast, the aortas exhibiting the most dilated/aneurysmal phenotypes ($ApoE^{-/-}$ + HT, figure 1*j*; $Fbn1^{mgR/mgR}$, figure 1*m*; $Fbln4^{SMKO}$, figure 1*n*) appear stiffer relative to controls (figure 1*a*–*d*). Such stiffening typically results from a combination of elastic fibre fragmentation and collagen deposition and remodelling, the latter dominating in $ApoE^{-/-}$ + HT ascending aortas (figure 1*t*) and the former in $Fbn1^{mgR/mgR}$ and $Fbln4^{SMKO}$ aortas (figure 1*w*,*x*), where several regions within the media are devoid of elastic fibres, including the inner layers. Interestingly, although the absence of fibulin-5 does not predispose to TAAs (figure 1*h*), fragmented elastic laminae are visible in the

Table 1. Physiological data (mean ± s.e.m.) for the four groups that constituted our control mice (pooled hereafter) and the eight groups of mutant/pharmacologically treated mice. *Myh11*$^{+/+}$, *Fbln5*$^{+/+}$ and *Fbn1*$^{+/+}$ were generated as a by-product by breeding heterozygous mutant mice to produce homozygous mutant mice; wild-type (WT) refers to inbred mice maintained through sibling matings. Background, age, body mass and blood pressure (systolic/diastolic) are indicated for each group. Differences in background and age were dictated by prior individual studies that focused on the effect of each mutation [16–18,20,22]. The value of systolic pressure was adjusted (adj) to conscious mouse conditions depending on the protocol and apparatus used for data acquisition [23,24]. Note that elastase was applied to WT C57BL/6J ascending aortas; hence, donor mice are not listed as a separate group. Note: C, indwelling (aortic) polyethylene catheter in the conscious mouse; M, Millar ascending aortic catheter in the anaesthetized mouse (1.2% isoflurane); S, Scisense ascending aortic catheter in the anaesthetized mouse (1.5% isoflurane); T, non-invasive tail cuff method in the conscious mouse. By mild phenotype, we mean that the aortic properties were nearly, though not precisely, normal.

	background	age (weeks)	body mass (g)	$P_{sys/dias}$ (mm Hg)	$P_{sys,adj}$ (mm Hg)	aortic phenotype
controls						
Myh11$^{+/+}$	C57BL/6;129SvJ	27.3 ± 0.5	27.4 ± 1.9	124 ± 3/91 ± 3 – T	125	normal
Fbln5$^{+/+}$	C57BL/6;129/SvEv	21.2 ± 0.2	31.9 ± 1.8	120 ± 6/84 ± 6 – T	120	normal
Fbn1$^{+/+}$	C57BL/6;Sv129;SW	8.5 ± 0.1	29.0 ± 1.2	124 ± 1/91 ± 1 – C	124	normal
wild-type	C57BL/6J	15.2 ± 0.1	28.9 ± 0.7	127 ± 1/97 ± 2 – T	128	normal
mutants						
Myh11$^{R247C/R247C}$	C57BL/6;129SvJ	26.0 ± 0.8	29.0 ± 1.5	117 ± 3/82 ± 1 – T	117	mild
Fbln5$^{-/-}$	C57BL/6;129/SvEv	21.2 ± 0.3	30.5 ± 1.4	121 ± 7/85 ± 7 – T	122	stiff/tortuous
Myh11$^{R247C/R247C}$ + HT	C57BL/6;129SvJ	26.9 ± 0.6	23.6 ± 1.1	186 ± 7/143 ± 12 – T	189	dissection prone
ApoE$^{-/-}$ + HT	C57BL/6J	21.9 ± 1.3	31.2 ± 0.7	186 ± 3/141 ± 2 – T	189	dilated/thickened
Tgfbr2$^{f/f}$ + Tmx	backbred to C57BL/6	8.1 ± 0.1	21.8 ± 0.5	93 ± 2/70 ± 2 – M	109	dissection prone
Tsc1$^{f/f}$ + Tmx	backbred to C57BL/6	12.3 ± 0.1	28.0 ± 0.5	83 ± 2/63 ± 2 – M	97	aneurysm prone
Fbn1$^{mgR/mgR}$	C57BL/6;Sv129;SW	8.8 ± 0.2	30.2 ± 0.4	131 ± 5/88 ± 4 – C	132	aneurysmal
Fbln4^{SMKO}	C57BL/6J;129SvEv	13.1 ± 0.2	17.2 ± 0.4	107 ± 3/56 ± 1 – S	131	aneurysmal

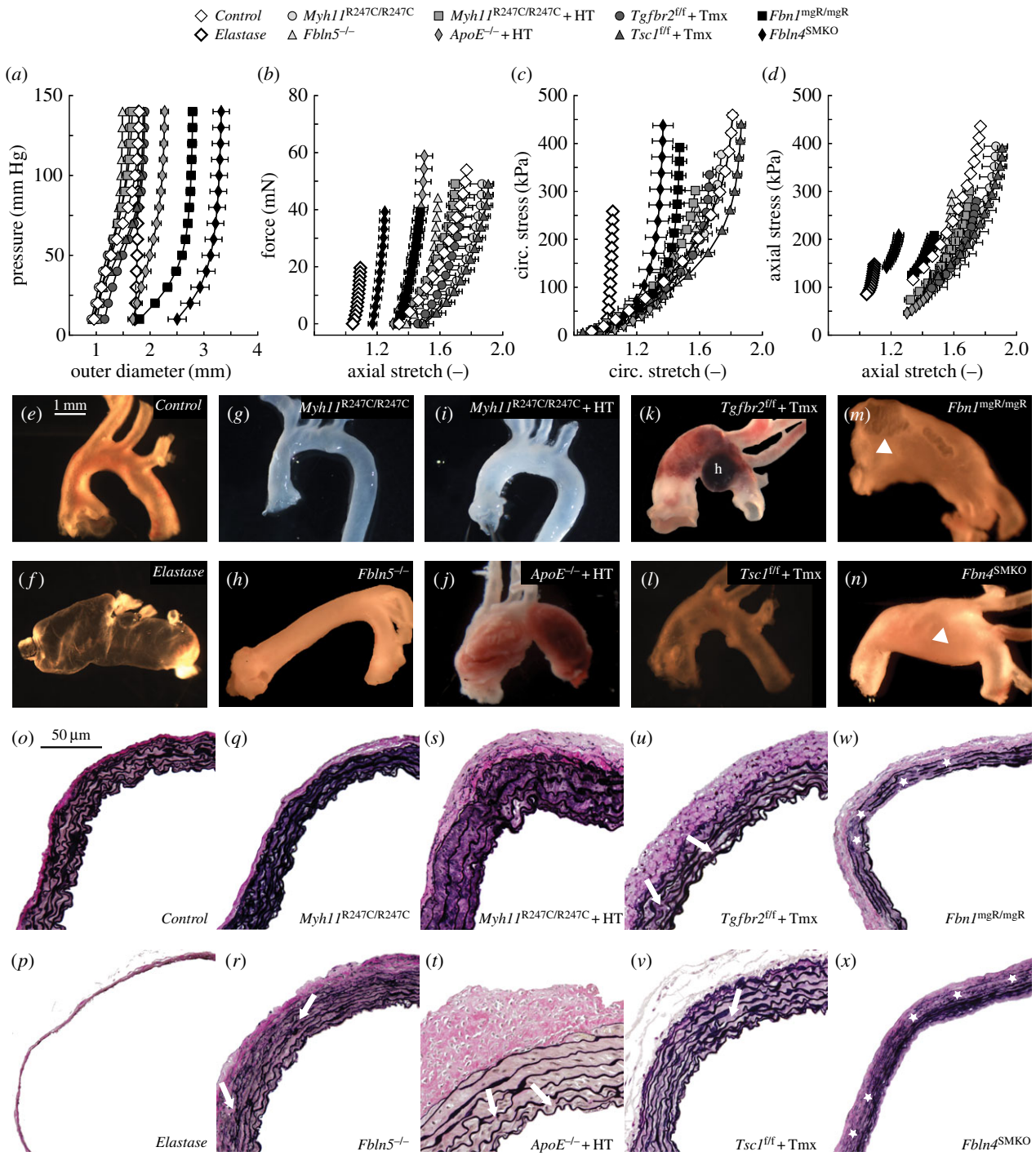

Figure 1. Biaxial mechanical data (*a–d*), gross anatomy (*e–n*) and VVG-stained cross sections (*o–x*) from control, elastase-exposed controls and mutant/treated ascending aortas suggest a correlation between the degree and location of elastic fibre loss (star symbols, *w,x*) or fragmentation (white arrows, *r,t,u,v*), the decrease in circumferential distension (*a,c*) and axial extension (*b,d*) and the likelihood of aneurysm development/progression (*e–n*). White arrowheads in (*m,n*) indicate marked aneurysms. The lower-case letter h in (*k*) shows an intramural haematoma. Notice that elastase-exposed vessels do not mimic *per se* any *in vivo* condition, but they reveal the effect of a complete loss of competent elastic fibres (*p*) without concomitant matrix remodelling. As such, control and elastase-exposed control vessels define bounds for the stress–stretch responses in the circumferential direction (*c*). Note: elastase-exposed control, *Fbn1*$^{mgR/mgR}$ and *Fbln4*^{SMKO} ascending aortas were perfusion-fixed (luminal pressure $<$100 mm Hg for the elastase-treated vessels, $<$20 mm Hg for the aneurysmal vessels) at their *in vivo* axial length to avoid collapse due to the large diameter. Other vessels were fixed in the unloaded state.

outer layers of the media (figure 1*r*) and the mechanical behaviour appears to be intermediate between the groups of mild (e.g. *Tgfbr2*$^{f/f}$ + Tmx) and severe (e.g. *Fbn1*$^{mgR/mgR}$) aneurysmal models (figure 1*a–d*). Collectively, these data may suggest that any defect in the elastic fibres can compromise mechanical functionality, but loss of inner elastic lamellae may be needed to enable aneurysmal formation. In the absence of larger datasets indicating differential elastic fibre organization within different laminae across the arterial wall, there is a need to understand better the potential mechanical advantage of inner versus outer elastic layers.

Figure 2 compares systolic values of eight important mechanical metrics across all 10 mouse models: biaxial stretch (figure 2*a,b*), wall stress (figure 2*c,d*) and intrinsic material stiffness (figure 2*e,f*) plus elastic energy storage (figure 2*g*) and distensibility (figure 2*h*), a measure of structural stiffness. See also electronic supplementary material, table S1. We assessed potential correlations between values

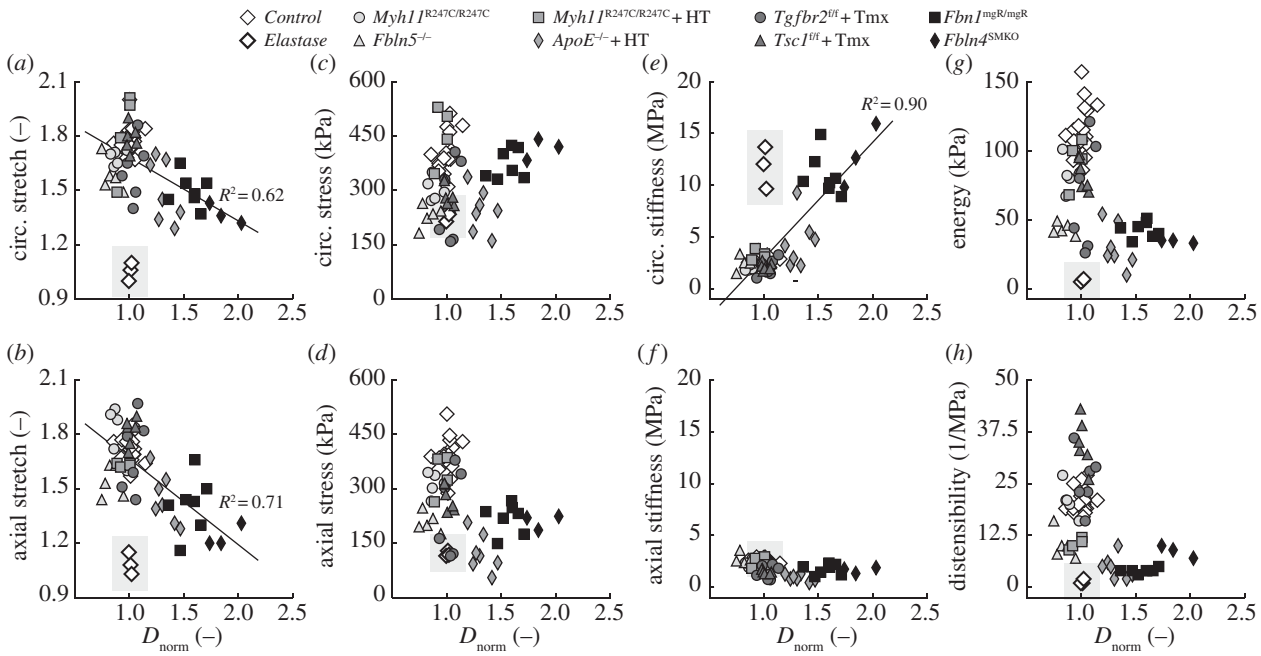

Figure 2. Mechanical metrics of stretch (*a,b*), wall stress (*c,d*), stiffness (*e,f*), energy (*g*) and distensibility (*h*) are plotted as a function of D_{norm} (i.e. the outer diameter at systole normalized to the average diameter at systole for the control group) for all specimens. Note that an aneurysm is defined by $D_{norm} > 1.5$. The circumferential (*a*) and axial (*b*) stretch at systole progressively decrease as the ascending aorta dilates. Whereas *material* circumferential stiffness (*e*) increases with dilatation, the distensibility, a common metric of *structural* stiffness, does not correlate with the propensity towards aneurysm formation (*h*). Overall, vessels from mutant mice reach normal or lower-than-normal values of both circumferential (*c*) and axial (*d*) stress as well as axial stiffness (*f*). Finally, all of the genetic mutations and pharmacological treatments considered in this study decrease the elastic energy stored at systole, thus impairing the ability of the aorta to perform a key mechanical function (*g*). Notice that data from elastase-exposed controls (thick white diamonds embedded within the grey shaded area) serve as good comparisons since there is no associated cell-mediated remodelling following the structural and material insult; these data were not included in the regressions, however.

of each of these eight metrics (*y*-axes) and the degree of aortic dilatation (*x*-axis, that is, outer diameter at systole relative to that for controls—D_{norm}); electronic supplementary material, figure S1, shows the same data though organized as group means ± s.e.m. There are five notable findings. First, increased dilatation of the ascending aorta across models correlates well with a decrease in both circumferential (figure 2*a*; regression line: $y = -0.35x + 2.03$, $R^2 = 0.62$) and axial (figure 2*b*; regression line: $y = -0.47x + 2.14$, $R^2 = 0.71$) stretch at systole, with the enlarged $ApoE^{-/-}$ + HT ($D_{norm} > 1.3$) and aneurysmal $Fbn1^{mgR/mgR}$ and $Fbln4^{SMKO}$ ($D_{norm} > 1.5$) ascending aortas being least deformable. A reduced value of axial stretch can be mechanically protective for it can unload the vessel biaxially, yet extreme decreases could be detrimental by predisposing to tortuosity depending on perivascular tethering and tethering at the end of the aortic segment. The data in figure 2*b* are consistent with an increasing propensity for lengthening with increasing aneurysmal dilatation. Second, biaxial wall stresses are either nearly normal or reduced in all mutant and pharmacologically treated models (figure 2*c,d*), due in part to increased wall thickness (electronic supplementary material, table S1) and decreased axial stretch (figure 2*b*). This finding suggests that circumferential wall stress, not stretch, is controlled reasonably well during aneurysmal enlargement.

Third, circumferential material stiffness increases proportionally with the degree of dilatation, reaching its highest values in enlarged $ApoE^{-/-}$ + HT and aneurysmal $Fbn1^{mgR/mgR}$ and $Fbln4^{SMKO}$ aortas (figure 2*e*; regression line: $y = 11.19x - 8.22$, $R^2 = 0.90$). Importantly, the aneurysmal vessels exhibit values of circumferential material stiffness similar to those for elastase-exposed aortas, in which there is no matrix remodelling. This finding suggests an inability by intramural cells to mechanoregulate the matrix circumferentially, even though axial material stiffness is similar to or less than normal in all the mutant/treated models (figure 2*f*). Fourth, the combination of increased wall thickness and circumferential material stiffness in the three dilated/aneurysmal models leads to a significant increase in structural stiffness, as revealed by reduced values of distensibility *D* (figure 2*h*). Nevertheless, *D* does not correlate with aneurysmal dilatation because the non-aneurysm-prone $Fbln5^{-/-}$ and $Myh11^{R247C/R247C}$ + HT ascending aortas also exhibit marked reductions in distensibility.

Fifth, a common finding for all of the genetic mutations and pharmacological treatments considered is a decrease in elastic energy storage (figure 2*g*; electronic supplementary material, figure S2), which reflects a reduced mechanical functionality because a key role of the aorta is to use energy stored during systole to augment blood flow during diastole. Once again, enlarged $ApoE^{-/-}$ + HT and aneurysmal $Fbn1^{mgR/mgR}$ and $Fbln4^{SMKO}$ aortas have marked reductions in energy storage capacity, but so too the $Fbln5^{-/-}$ aortas that do not become aneurysmal. A complementary finding was seen for energy dissipation, with dilated vessels, in addition to the non-dilated $Fbln5^{-/-}$ aortas, dissipating more energy upon cyclic deformations than controls (electronic supplementary material, table S1). Consistent with their nearly normal appearance and microstructure (cf. figure 1*g,i,q,s*), normotensive and hypertensive $Myh11^{R247C/R247C}$ ascending aortas store only slightly less energy than controls, which exhibited the highest energy storage (115 kPa), while the elastase-exposed vessels exhibited the lowest storage (6 kPa), thus bounding the behaviours. Interestingly, $Tgfbr2^{f/f}$ + Tmx and $Tsc1^{f/f}$ + Tmx ascending aortas, which are prone to aneurysms or dissections, exhibit different

levels of energy storage: close to normal by the $Tsc1^{f/f}$ + Tmx model (despite slight hypotension; table 1) but reduced by the $Tgfbr2^{f/f}$ + Tmx model (despite normotension). Hence, despite having important effects on the biomechanics, elastic energy storage and dissipation do not correlate with aneurysms or their propensity.

Whereas we sought correlations between any of these eight important mechanical metrics and aortic dilatation (figure 2; electronic supplementary material, figure S1), noting that uncontrolled hypertension is a key risk factor for aneurysms, we similarly examined possible correlations with the group-specific *in vivo* systolic pressure. No such correlation was found for the mechanical or geometric metrics, including wall thickness and thickness : radius ratio (electronic supplementary material, figure S3). For evaluations of potential effects due to genetic background (e.g. C57BL/6J versus C57BL/6;129SvEv), methods for inducing the mutation (e.g. germ-line versus Cre-lox induction) and chronological age, see [19], wherein it is noted that the method used to induce a mutation can have a small effect on some mechanical metrics. Finally, for completeness, note that electronic supplementary material, table S2, lists values of the model parameters used in the constitutive relation to describe the behaviour of the ascending aorta for each of the 10 mouse models.

4. Discussion

Estimates of arterial wall properties *in vivo* necessarily focus on circumferential metrics of structural stiffness such as the so-called distensibility D. Nevertheless, changes in axial properties are critically important to wall mechanics, often manifesting as early or dramatic changes [25]. Data should thus be collected and compared for biaxial wall stress and material stiffness as well as for elastic energy storage because different metrics provide different insights into the mechanics and mechanobiology [26]. Such data are best inferred *in vitro* from multiple cyclic pressure–diameter and axial force–length protocols performed on vessels having a near native geometry and exposed to *in vivo* values of loads at body temperature. This was our approach. Although aneurysms manifest in both the ascending and descending thoracic aorta, the former present a greater clinical concern. Moreover, Marfan syndrome manifests primarily in the ascending aorta, near the aortic root. Hence, we focused on the ascending region even though similar studies are warranted for the descending thoracic aorta. We also considered models used to study conditions of thoracic aorta, but did not wait until a particular disease severity manifested. In this way, we could study potential propensity, which is critical from a clinical perspective of prognosis and treatment planning.

In addition to our newly collected biaxial data on $Tsc1^{f/f}$ + Tmx, $ApoE^{-/-}$ + HT, $Fbln4^{SMKO}$, elastase-exposed and control ascending aortas, we previously reported similar data for five other models [16–18,20]: $Myh11^{R247C/R247C}$, $Myh11^{R247C/R247C}$ + HT, $Tgfbr2^{f/f}$ + Tmx, $Fbn1^{mgR/mgR}$ and $Fbln5^{-/-}$. Collectively, these 10 models represent diverse aortic phenotypes (table 1), ranging from normal (*Control*) to a stiffer and lengthened aorta without a propensity to form aneurysms ($Fbln5^{-/-}$), a mild phenotype ($Myh11^{R247C/R247C}$) with little dilatation that is yet vulnerable to dissections when rendered hypertensive ($Myh11^{R247C/R247C}$ + HT), a moderate phenotype at young ages with some dilatation that develops aneurysms later in life ($Tsc1^{f/f}$ + Tmx), a dissection-prone vessel ($Tgfbr2^{f/f}$ + Tmx), a vessel with dramatic dilatation despite wall thickening ($ApoE^{-/-}$ + HT) and ultimately ones with marked aneurysmal development ($Fbn1^{mgR/mgR}$ and $Fbln4^{SMKO}$). Recall that human TAAs similarly associate with mutations in genes that code for the elastin-associated glycoproteins fibrillin-1 and fibulin-4 [2], but typically not fibulin-5 (cf. [21,27]). These glycoproteins contribute to elastogenesis and long-term mechanical stability, that is, formation and subsequent normally long half-life of elastic fibres [28]. Human TAAs also associate with mutations to genes that code smooth muscle cell contractile proteins, including smooth muscle myosin heavy chain and smooth muscle α-actin [1]. Contractile proteins can contribute both to vessel level contractility and cell level mechanosensing and mechanoregulation of the extracellular matrix. Dysfunctional sensing and regulation of matrix appear to be consistent across many TAAs [4,5]. TAAs also associate with mutations to genes that code transforming growth factor receptors [2]. That dysregulated transforming growth factor-β, or its signalling, plays a role in TAAs is unquestioned, but significant controversy remains in regard to precise roles. Tuberous sclerosis similarly associates with aortic disease [29,30], but there has not been any prior detailed study of its mechanical consequences. Finally, although the high-dose angiotensin II infusion mouse model does not mimic a specific human condition, it causes enlargements of the ascending aorta with a phenotype similar to that in fibrillin-1-deficient mice [15,31]. Given that angiotensin II also raises blood pressure, recall that uncontrolled hypertension is an additional risk factor for TAAs [1]. The mice considered included two different hypertensive models, angiotensin II infused and a high-salt diet with L-NAME to block nitric oxide bioavailability. Thus, our examination of this collection of 10 mouse models was motivated by human conditions and risk factors even though one must be cautious when attempting to translate results from mice to humans. There is, therefore, a pressing need for more data on human lesions and consistent comparisons across multiple syndromic and non-syndromic cases. Nevertheless, general results across multiple mouse models have potential to provide insight well beyond that afforded by a single model.

Our findings suggest two primary conclusions. First, increased circumferential material stiffness correlates well with the degree of aortic dilatation ($R^2 = 0.90$; figure 2*e*; electronic supplementary material, figure S1*e*). This finding implies that transient elevations in blood pressure, as in strenuous activities, could generate larger increases in wall stress in aneurysmal than in normal ascending aortas, which could promote further expansion or rupture of a compromised vessel [32]. This finding further implies a dysfunctional cellular sensing and/or regulation of the extracellular matrix, which supports recent suggestions inferred in the absence of detailed mechanical data [4,33,34]. In particular, although the present data cannot delineate cause and consequence, increases in circumferential stiffness in the aneurysmal phenotypes to levels comparable to those in aortas exposed acutely to elastase reveal that the intramural cells did not deposit or remodel the collagen properly *in vivo*. Indeed, whereas computational models show that an increased deposition of appropriately formed circumferential collagen fibres can help slow or arrest aneurysmal

expansion [35], this was not seen in our TAA mouse models. Given that many previous reports suggest that intramural cells seek to establish, maintain and restore normal values of circumferential material stiffness in health as well as many disease conditions [20,26,28,36], which seems mechanobiologically favourable, there is a pressing need to elucidate the molecular mechanisms of dysfunctional mechanocontrol of matrix in aneurysms of the ascending aorta.

Second, decreased mechanical functionality of the aorta need not reflect or contribute directly to aneurysmal dilatation. Although aortic distensibility is a commonly measured clinical metric of stiffness (the lower the value of D, the higher the structural stiffness), and it is elevated in Marfan syndrome patients among others [37,38], our findings reveal that D does not correlate with aneurysmal progression. Hence, distensibility should not be used clinically as an indicator of ascending aortic aneurysm or its risk. Similarly, loss of energy storage capability, via either compromised elastic fibre integrity [20] or an excessive deposition of collagen that prevents competent elastic fibres from deforming and storing energy [39], is not diagnostic of TAAs. Given that decreased distensibility and energy storage are also characteristic of arterial ageing and hypertension, these two conditions are likely exaggerating risk factors for aneurysms, not disease initiators *per se*. In particular, a general loss of distensibility and energy storage in central arteries can adversely increase pulse wave velocities and thus augment central pulse pressures, which could indirectly exacerbate aneurysmal progression or promote dissection or rupture. We emphasize, however, that this study focused on aneurysmal dilation, not material failure. It is likely that dissection and rupture result from different mechanisms and there is equal need to study these two failure modes, which arise when local haemodynamically induced wall stress exceeds strength. Indeed, there is also a general need to understand the natural history of thoracic disease within the broader context of the haemodynamics, not just local wall mechanics or local molecular mechanisms. Only by combining the genetics, cell biology, imaging and comprehensive biomechanical analyses (e.g. fluid-solid-growth modelling) will we understand these disease conditions fully.

Notwithstanding the new insight gained—based on a consistent analysis of both newly acquired and previously reported biomechanical data—there are limitations inherent to our retrospective study. The 10 datasets were collected at different times and for different purposes; hence, the experimental protocols were similar but not identical. For some of the mouse models, the group-specific mean value of systolic blood pressure was obtained by averaging measurements over each mouse within the group; for other models, it was based either on additional mice that were not used for mechanical testing or mean values from the literature. Hence, we could not assess directly the relation between blood pressure and individual mechanical metrics. Similar considerations hold for other possible contributors. Hence, the effect of such factors on the computed mechanical metrics could not be assessed with more sophisticated regression models. Based on our previous results for potential control mice [19], however, it appears that the degree of aortic dilatation (D_{norm})—that is, the disease itself—is a stronger determinant of altered mechanics than other variables such as blood pressure, age and genetic background, at least within the limits of our study. Finally, each mouse model was analysed at a single prescribed time of interest, not based on longitudinal studies wherein disease progression was followed. There is clearly a need for longitudinal studies in mice, particularly since such studies are very difficult in humans. We conclude by submitting that considerable insight can be gleaned from mouse models of TAAs, but there is strong motivation for consistent comparisons across multiple models since no animal model phenocopies exactly the human disease.

Data accessibility. Material parameters and geometrical measures are provided in the electronic supplementary material.

Competing interests. We declare we have no competing interests.

Funding. This work was supported, in part, by grants from the National Institutes of Health (P01 HL110869 to D.M.M.; R01 HL126173 to F.R.; R01 CA034282 to D.B.R.; R01 HL106305 to H.Y.; and R03 EB021430, R01 HL105297 and U01 HL116323 to J.D.H.) and the National Marfan Foundation (to D.B.R., G.T. and J.D.H.).

Acknowledgements. We would like to thank Dr S. Wang, Dr L. Zilberberg and Mr G. Urquhart for the collection of some of the aortic tissue specimens that were discussed herein.

References

1. Milewicz DM, Guo DC, Tran-Fadulu V, Lafont AL, Papke CL, Inamoto S, Kwartler CS, Pannu H. 2008 Genetic basis of thoracic aortic aneurysms and dissections: focus on smooth muscle cell contractile dysfunction. *Annu. Rev. Genomics Hum. Genet.* **9**, 283–302. (doi:10.1146/annurev.genom.8.080706.092303)
2. Lindsay ME, Dietz HC. 2014 The genetic basis of aortic aneurysm. *Cold Spring Harb. Perspect. Med.* **4**, a015909. (doi:10.1101/cshperspect.a015909)
3. El-Hamamsy I, Yacoub MH. 2009 Cellular and molecular mechanisms of thoracic aortic aneurysms. *Nat. Rev. Cardiol.* **6**, 771–786. (doi:10.1038/nrcardio.2009.191)
4. Humphrey JD, Milewicz DM, Tellides G, Schwartz MA. 2014 Cell biology. Dysfunctional mechanosensing in aneurysms. *Science* **344**, 477–479. (doi:10.1126/science.1253026)
5. Humphrey JD, Schwartz MA, Tellides G, Milewicz DM. 2015 Role of mechanotransduction in vascular biology: focus on thoracic aortic aneurysms and dissections. *Circ. Res.* **116**, 1448–1461. (doi:10.1161/CIRCRESAHA.114.304936)
6. Sokolis DP, Kritharis EP, Giagini AT, Lampropoulos KM, Papadodima SA, Iliopoulos DC. 2012 Biomechanical response of ascending thoracic aortic aneurysms: association with structural remodelling. *Comput. Methods Biomech. Biomed. Eng.* **15**, 231–248. (doi:10.1080/10255842.2010.522186)
7. Pierce DM, Maier F, Weisbecker H, Viertler C, Verbrugghe P, Famaey N, Fourneau I, Herijgers P, Holzapfel GA. 2015 Human thoracic and abdominal aortic aneurysmal tissues: damage experiments, statistical analysis and constitutive modeling. *J. Mech. Behav. Biomed. Mater.* **41**, 92–107. (doi:10.1016/j.jmbbm.2014.10.003)
8. Martufi G, Gasser TC, Appoo JJ, Di Martino ES. 2014 Mechano-biology in the thoracic aortic aneurysm: a review and case study. *Biomech. Model. Mechanobiol.* **13**, 917–928. (doi:10.1007/s10237-014-0557-9)
9. Garcia-Herrera CM, Atienza JM, Rojo FJ, Claes E, Guinea GV, Celentano DJ, Garcia-Montero C, Burgos RL. 2012 Mechanical behaviour and rupture of normal and pathological human ascending aortic wall. *Med. Biol. Eng. Comput.* **50**, 559–566. (doi:10.1007/s11517-012-0876-x)
10. Azadani AN, Chitsaz S, Mannion A, Mookhoek A, Wisneski A, Guccione JM, Hope MD, Ge L, Tseng EE. 2013 Biomechanical properties of human ascending thoracic aortic aneurysms. *Ann. Thorac.*

Surg. **96**, 50–58. (doi:10.1016/j.athoracsur.2013.03.094)

11. Pereira L *et al.* 1999 Pathogenetic sequence for aneurysm revealed in mice underexpressing fibrillin-1. *Proc. Natl Acad. Sci. USA* **96**, 3819–3823. (doi:10.1073/pnas.96.7.3819)
12. Huang J, Davis EC, Chapman SL, Budatha M, Marmorstein LY, Word RA, Yanagisawa H. 2010 Fibulin-4 deficiency results in ascending aortic aneurysms: a potential link between abnormal smooth muscle cell phenotype and aneurysm progression. *Circ. Res.* **106**, 583–592. (doi:10.1161/CIRCRESAHA.109.207852)
13. Kuang SQ *et al.* 2012 Rare, nonsynonymous variant in the smooth muscle-specific isoform of myosin heavy chain, MYH11, R247C, alters force generation in the aorta and phenotype of smooth muscle cells. *Circ. Res.* **110**, 1411–1422. (doi:10.1161/CIRCRESAHA.111.261743)
14. Li W *et al.* 2014 Tgfbr2 disruption in postnatal smooth muscle impairs aortic wall homeostasis. *J. Clin. Invest.* **124**, 755–767. (doi:10.1172/JCI69942)
15. Daugherty A, Rateri DL, Charo IF, Owens AP, Howatt DA, Cassis LA. 2010 Angiotensin II infusion promotes ascending aortic aneurysms: attenuation by CCR2 deficiency in apoE$^{-/-}$ mice. *Clin. Sci. (Lond)* **118**, 681–689. (doi:10.1042/CS20090372)
16. Bellini C, Wang S, Milewicz DM, Humphrey JD. 2015 Myh11(R247C/R247C) mutations increase thoracic aorta vulnerability to intramural damage despite a general biomechanical adaptivity. *J. Biomech.* **48**, 113–121. (doi:10.1016/j.jbiomech.2014.10.031)
17. Ferruzzi J, Murtada SI, Li G, Jiao Y, Uman S, Ting MY, Tellides G, Humphrey JD. 2016 Pharmacologically improved contractility protects against aortic dissection in mice with disrupted transforming growth factor-beta signaling despite compromised extracellular matrix properties. *Arterioscler. Thromb. Vasc. Biol.* **36**, 919–927. (doi:10.1161/ATVBAHA.116.307436)
18. Bellini C, Korneva A, Zilberberg L, Ramirez F, Rifkin DB, Humphrey JD. 2016 Differential ascending and descending aortic mechanics parallel aneurysmal propensity in a mouse model of Marfan syndrome. *J. Biomech.* **49**, 2383–2389. (doi:10.1016/j.jbiomech.2015.11.059)
19. Bellini C, Ferruzzi J, Caulk AW, Li G, Tellides G, Humphrey JD. 2016 Biomechanical phenotyping the murine aorta: what is the best control? *J. Biomech. Eng.* **139**, 044501. (doi:10.1115/1.4035551)
20. Ferruzzi J, Bersi MR, Uman S, Yanagisawa H, Humphrey JD. 2015 Decreased elastic energy storage, not increased material stiffness, characterizes central artery dysfunction in fibulin-5 deficiency independent of sex. *J. Biomech. Eng.* **137**, 031007. (doi:10.1115/1.4029431)
21. Yanagisawa H, Davis EC, Starcher BC, Ouchi T, Yanagisawa M, Richardson JA, Olson EN. 2002 Fibulin-5 is an elastin-binding protein essential for elastic fibre development *in vivo*. *Nature* **415**, 168–171. (doi:10.1038/415168a)
22. Bellini C, Kristofik NJ, Bersi MR, Kyriakides TR, Humphrey JD. 2017 A hidden structural vulnerability in the thrombospondin-2 deficient aorta increases the propensity to intramural delamination. *J. Mech. Behav. Biomed. Mater.* **71**, 397–406. (doi:10.1016/j.jmbbm.2017.01.045)
23. Janssen BJ, De Celle T, Debets JJ, Brouns AE, Callahan MF, Smith TL. 2004 Effects of anesthetics on systemic hemodynamics in mice. *Am. J. Physiol. Heart Circ. Physiol.* **287**, H1618–H1624. (doi:10.1152/ajpheart.01192.2003)
24. Whitesall SE, Hoff JB, Vollmer AP, D'Alecy LG. 2004 Comparison of simultaneous measurement of mouse systolic arterial blood pressure by radiotelemetry and tail-cuff methods. *Am. J. Physiol. Heart Circ. Physiol.* **286**, H2408–H2415. (doi:10.1152/ajpheart.01089.2003)
25. Humphrey JD, Eberth JF, Dye WW, Gleason RL. 2009 Fundamental role of axial stress in compensatory adaptations by arteries. *J. Biomech.* **42**, 1–8. (doi:10.1016/j.jbiomech.2008.11.011)
26. Bersi MR, Ferruzzi J, Eberth JF, Gleason Jr RL, Humphrey JD. 2014 Consistent biomechanical phenotyping of common carotid arteries from seven genetic, pharmacological, and surgical mouse models. *Ann. Biomed. Eng.* **42**, 1207–1223. (doi:10.1007/s10439-014-0988-6)
27. Wang X *et al.* 2005 Decreased expression of fibulin-5 correlates with reduced elastin in thoracic aortic dissection. *Surgery* **138**, 352–359. (doi:10.1016/j.surg.2005.06.006)
28. Wagenseil JE, Mecham RP. 2009 Vascular extracellular matrix and arterial mechanics. *Physiol. Rev.* **89**, 957–989. (doi:10.1152/physrev.00041.2008)
29. Lendvay TS, Marshall FF. 2003 The tuberous sclerosis complex and its highly variable manifestations. *J. Urol.* **169**, 1635–1642. (doi:10.1097/01.ju.0000058253.40352.60)
30. Cao J *et al.* 2010 Thoracic aortic disease in tuberous sclerosis complex: molecular pathogenesis and potential therapies in Tsc2$^{+/-}$ mice. *Hum. Mol. Genet.* **19**, 1908–1920. (doi:10.1093/hmg/ddq066)
31. Tieu BC *et al.* 2009 An adventitial IL-6/MCP1 amplification loop accelerates macrophage-mediated vascular inflammation leading to aortic dissection in mice. *J. Clin. Invest.* **119**, 3637–3651. (doi:10.1172/JCI38308)
32. Elefteriades JA. 2008 Thoracic aortic aneurysm: reading the enemy's playbook. *Curr. Probl. Cardiol.* **33**, 203–277. (doi:10.1016/j.cpcardiol.2008.01.004)
33. Yamashiro Y *et al.* 2015 Abnormal mechanosensing and cofilin activation promote the progression of ascending aortic aneurysms in mice. *Sci. Signal.* **8**, ra105. (doi:10.1126/scisignal.aab3141)
34. Cook JR *et al.* 2015 Dimorphic effects of transforming growth factor-beta signaling during aortic aneurysm progression in mice suggest a combinatorial therapy for Marfan syndrome. *Arterioscler. Thromb. Vasc. Biol.* **35**, 911–917. (doi:10.1161/ATVBAHA.114.305150)
35. Wilson JS, Baek S, Humphrey JD. 2013 Parametric study of effects of collagen turnover on the natural history of abdominal aortic aneurysms. *Proc. Math. Phys. Eng. Sci.* **469**, 20120556. (doi:10.1098/rspa.2012.0556)
36. Shadwick RE. 1999 Mechanical design in arteries. *J. Exp. Biol.* **202**, 3305–3313.
37. Akazawa Y *et al.* 2016 Decreased aortic elasticity in children with Marfan syndrome or Loeys-Dietz syndrome. *Circ. J.* **80**, 2369–2375. (doi:10.1253/circj.CJ-16-0739)
38. Groenink M, de Roos A, Mulder BJ, Spaan JA, van der Wall EE. 1998 Changes in aortic distensibility and pulse wave velocity assessed with magnetic resonance imaging following beta-blocker therapy in the Marfan syndrome. *Am. J. Cardiol.* **82**, 203–208. (doi:10.1016/S0002-9149(98)00315-4)
39. Bersi MR, Bellini C, Wu J, Montaniel KR, Harrison DG, Humphrey JD. 2016 Excessive adventitial remodeling leads to early aortic maladaptation in angiotensin-induced hypertension. *Hypertension* **67**, 890–896. (doi:10.1161/HYPERTENSIONAHA.115.06262)